PHYSICAL REVIEW A **81**, 051605(R) (2010)

Pairing and condensation in a resonant Bose-Fermi mixture

Elisa Fratini and Pierbiagio Pieri

Sezione di Fisica, Scuola di Scienze e Tecnologie, Università di Camerino and CNISM, Via Madonna delle Carceri 9, I-62032 Camerino, Italy

(Received 12 January 2010; revised manuscript received 15 March 2010; published 17 May 2010)

We study by diagrammatic means a Bose-Fermi mixture, with boson-fermion coupling tuned by a Fano-Feshbach resonance. For increasing coupling, the growing boson-fermion pairing correlations progressively reduce the boson condensation temperature and make it eventually vanish at a critical coupling. Such quantum critical point depends very weakly on the population imbalance and, for vanishing boson densities, coincides with that found for the polaron-molecule transition in a strongly imbalanced Fermi gas, thus bridging two quite distinct physical systems.

DOI: 10.1103/PhysRevA.81.051605 PACS number(s): 03.75.Hh, 05.30.Jp, 03.75.Ss, 67.85.−d

One of the main reasons behind the recent great interest in ultracold gases is the possibility of reproducing physical systems relevant to other areas in physics, with a flexibility and a degree of tunability of physical parameters which is unimaginable in the original system of interest. The very same flexibility can also be used, however, to construct novel physical systems. A noticeable example of such novel systems, namely, resonant Bose-Fermi mixtures, is at issue here. We are interested in particular in the competition between boson-fermion pairing correlations and bosonic condensation, occuring in a mixture of single-component bosons and fermions when the boson-fermion pairing is made progressively stronger by means of a Fano-Feshbach resonance.

Initial theoretical studies of ultracold Bose-Fermi mixtures considered nonresonant systems [1], where boson-fermion pairing is irrelevant, and studied, within mean field, the tendency toward collapse or phase separation (as motivated by the first experimental results on nonresonant Bose-Fermi mixtures [2]). Bose-Fermi mixtures in the presence of a Fano-Feshbach resonance have been subsequently considered in [3–9], mostly for *narrow* resonances [3,6,8] and/or in specific contexts (such as optical lattices, reduced dimensionality, zero temperature, or vanishing density of one species) [4,5,7,9].

Most current experiments on Bose-Fermi mixtures [10–14] appear, however, to be closer to the case of a *broad* resonance, which is characterized by the smallness of the effective range parameter r_0 of the interaction potential with respect to both the average interparticle distance and the scattering length [15]. Under these conditions, the resonant Bose-Fermi mixture is accurately described by a *minimal* Hamiltonian, made just by bosons and fermions mutually interacting via an attractive point-contact potential. This Hamiltonian is simpler and more "fundamental" in character than its counterpart for a narrow resonance because of the absence of any other parameter besides the strength of the boson-fermion interaction.

We thus consider the following (grand-canonical) Hamiltonian:

$$H = \sum_s \int d\mathbf{r}\psi_s^\dagger(\mathbf{r})\left(-\frac{\nabla^2}{2m_s} - \mu_s\right)\psi_s(\mathbf{r}) + v_0 \int d\mathbf{r}\psi_B^\dagger(\mathbf{r})\psi_F^\dagger(\mathbf{r})\psi_F(\mathbf{r})\psi_B(\mathbf{r}). \quad (1)$$

Here $\psi_s^\dagger(\mathbf{r})$, creates a particle of mass m_s and chemical potential μ_s at spatial position $\mathbf{r}$, where $s = B, F$ indicates the boson and fermion atomic species, respectively, while v_0 is the bare strength of the contact interaction (we set $\hbar = k_B = 1$ throughout this article). Ultraviolet divergences arising from the use of a contact interaction in (1) are eliminated, as for two-component Fermi gases [16], by expressing the bare interaction v_0 in terms of the boson-fermion scattering length a via the (divergent) expression $1/v_0 = m_r/(2\pi a) - \int 2m_r/\mathbf{k}^2 d\mathbf{k}/(2\pi)^3$, where $m_r = m_B m_F/(m_B + m_F)$ is the reduced mass.

The Hamiltonian (1) does not contain explicitly the boson-boson interaction. Provided it is repulsive and nonresonant, this interaction yields in fact a mean-field shift, which is equivalent to a redefinition of the boson chemical potential (attractive boson-boson interactions would lead to mechanical instability and are excluded from our consideration). S-wave interaction between fermions is finally excluded by the Pauli principle.

The effective coupling strength in the many-body system is determined by comparing the boson-fermion scattering length a with the average interparticle distance $n^{-1/3}$ (with $n = n_B + n_F$, where n_B and n_F are the boson and fermion particle number density, respectively). In particular, we will use the same dimensionless coupling strength $(k_F a)^{-1}$ normally used for two-component Fermi gases, where the wave vector $k_F \equiv (3\pi^2 n)^{1/3}$ [note that k_F coincides with the noninteracting Fermi wave vector $k_F^0 = (6\pi^2 n_F)^{1/3}$ only for $n_B = n_F$].

The expected behavior of the system is clear in the two opposite limits of the boson-fermion coupling. In the weak-coupling limit, where the scattering length a is small and negative [such that $(k_F a)^{-1} \ll -1$], the two components will behave essentially as ideal gases. Bosons will condense at $T_c = 3.31 n_B^{2/3}/m_B$, while fermions will fill out (at sufficienty low temperature) a Fermi sphere with radius k_F^0, the chemical potentials μ_B and μ_F being modified with respect to their noninteracting values by the mean-field shifts $2\pi n_F a/m_r$ and $2\pi n_B a/m_r$, respectively. In the opposite strong-coupling limit, where a is small and positive [such that $(k_F a)^{-1} \gg 1$], bosons will pair with fermions to form tightly bound fermionic molecules, with binding energy $\epsilon_0 = 1/(2m_r a^2)$. In particular, in systems where $n_B \leqslant n_F$, on which we focus in the present article, all bosons will eventually pair with fermions into molecules (composite fermions), suppressing condensation completely.

In analogy with the BCS-BEC crossover problem in a two-component Fermi gas [16], the choice of the self-energy diagrams will be guided by the criterion that a single set of diagrams should recover the correct physical description of

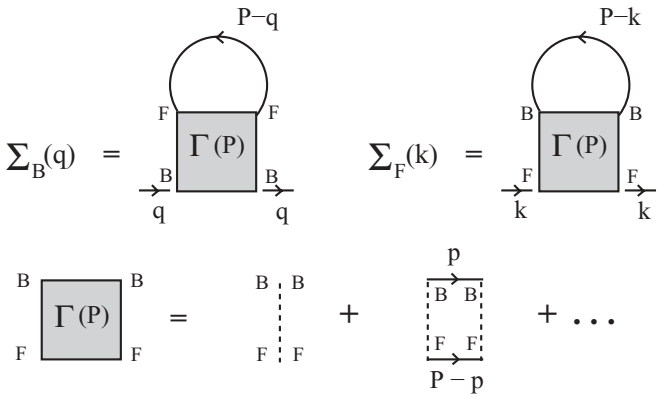

FIG. 1. T-matrix diagrams for the fermionic and bosonic self-energies in the normal phase. Full lines represent bare bosonic (BB) and fermionic (FF) Green's functions. Broken lines represent bare boson-fermion interactions v_0.

the preceding two opposite limits. In the *normal* phase above the condensation critical temperature T_c, to which we restrict in the present article, this condition is met (as we see below) by the T-matrix choice of diagrams represented in Fig. 1, yielding the expressions

$$\Sigma_B(q) = -\frac{1}{\beta}\int \frac{d\mathbf{P}}{(2\pi)^3}\sum_m G_F^0(P-q)\Gamma(P), \tag{2}$$

$$\Sigma_F(k) = \frac{1}{\beta}\int \frac{d\mathbf{P}}{(2\pi)^3}\sum_m G_B^0(P-k)\Gamma(P) \tag{3}$$

for the bosonic and fermionic self-energies Σ_B and Σ_F, where $G_B^0(q) = [i\omega_\nu - \xi_B(\mathbf{q})]^{-1}$ and $G_F^0 = [i\omega_n - \xi_F(\mathbf{k})]^{-1}$ are the corresponding bare Green's functions, while $\Gamma(P)$ is the many-body T-matrix:

$$\Gamma(P) = -\left\{\frac{m_r}{2\pi a} + \int\frac{d\mathbf{p}}{(2\pi)^3} \times \left[\frac{1-f[\xi_F(\mathbf{P}-\mathbf{p})]+b[\xi_B(\mathbf{p})]}{\xi_F(\mathbf{P}-\mathbf{p})+\xi_B(\mathbf{p})-i\Omega_m} - \frac{2m_r}{\mathbf{p}^2}\right]\right\}^{-1}. \tag{4}$$

In the preceding expressions, $q = (\mathbf{q},\omega_\nu)$, $k = (\mathbf{k},\omega_n)$, $P = (\mathbf{P},\Omega_m)$, where $\omega_\nu = 2\pi\nu/\beta$ and $\omega_n = (2n+1)\pi/\beta$, $\Omega_m = (2m+1)\pi/\beta$ are bosonic and fermionic Matsubara frequencies, respectively ($\beta = 1/T$ being the inverse temperature and ν,n,m integer), while $f(x)$ and $b(x)$ are the Fermi and Bose distribution functions and $\xi_s(\mathbf{p}) = \mathbf{p}^2/(2m_s) - \mu_s$. The preceding self-energies determine finally the dressed Green's functions $G_s^{-1} = G_s^{0\,-1} - \Sigma_s$ entering the particle numbers equations:

$$n_B = -\int\frac{d\mathbf{q}}{(2\pi)^3}\frac{1}{\beta}\sum_\nu G_B(\mathbf{q},\omega_\nu)\,e^{i\omega_\nu 0^+}, \tag{5}$$

$$n_F = \int\frac{d\mathbf{k}}{(2\pi)^3}\frac{1}{\beta}\sum_n G_F(\mathbf{k},\omega_n)\,e^{i\omega_n 0^+}. \tag{6}$$

Equations (2)–(6) fully determine the thermodynamic properties of the Bose-Fermi mixture in the normal phase. This phase is characterized by the condition $\mu_B - \Sigma_B(q=0) < 0$; upon lowering the temperature, condensation will then occur when $\mu_B = \Sigma_B(q=0)$ [17].

Analytic results can be obtained in the two opposite limits of the boson-fermion coupling [18]. For weak coupling, $\Gamma(P) \simeq -\frac{2\pi a}{m_r}$, yielding $\Sigma_B \simeq 2\pi n_F a/m_r$ and $\Sigma_F \simeq 2\pi n_B a/m_r$, in accordance with the expected mean-field shifts. For strong coupling, $\Gamma(P)$ gets instead proportional to the molecular propagator,

$$\Gamma(P) \simeq -\frac{2\pi}{m_r^2 a}\frac{1}{i\Omega_m - \frac{\mathbf{P}^2}{2M} + \mu_M}, \tag{7}$$

where $\mu_M \equiv \mu_B + \mu_F + \epsilon_0$ defines the molecular chemical potential and $M = m_B + m_F$. Insertion of this propagator in Eqs. (2)–(6) leads, for $n_B < n_F$, to $\mu_M \simeq (6\pi^2 n_B)^{2/3}/2M$, $\mu_F \simeq [6\pi^2(n_F - n_B)]^{2/3}/2m_F$, and $\mu_B \simeq -\epsilon_0$, as expected when all bosons pair with fermions.

For intermediate values of the boson-fermion coupling, Eqs. (2)–(6) need to be solved numerically. The results for the condensation critical temperature T_c vs the boson-fermion dimensionless coupling $(k_F a)^{-1}$ are presented in Fig. 2 for a mixture with $m_B = m_F$ at several values of density imbalance. [19] All curves start in weak coupling from the corresponding noninteracting values and decrease monotonically for increasing coupling due to the growing pairing correlations, which tend to deplete the zero-momentum mode and distribute the bosons over a vast momentum region, as required to build the internal molecular wave function. The critical temperature vanishes eventually at a critical coupling, corresponding to a quantum critical point which separates a phase with a condensate from a phase where molecular correlations are so strong they deplete the condensate completely.

Remarkably, the critical coupling value depends very weakly on the degree of density imbalance: All curves terminate in the narrow region $1.6 < (k_F a)^{-1} < 1.8$. In this respect, it is interesting to consider the limit $n_B \to 0$, where the critical coupling can be calculated independently by solving the problem of a single boson immersed in a Fermi sea. This is actually the same as a spin-down fermion surrounded by a Fermi sea of spin-up fermions, since for a single particle the statistics is immaterial. The critical coupling reduces thus to that for the polaron-to-molecule transition, recently studied in the context of strongly imbalanced *two-component Fermi gases* [20–23]. In particular, we have verified analytically

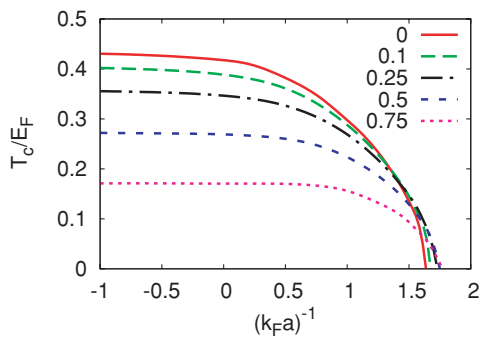

FIG. 2. (Color online) Critical temperature (in units of $E_F = k_F^2/2m_F$) for condensation of bosons vs the boson-fermion coupling $(k_F a)^{-1}$ for different values of the density imbalance $(n_F - n_B)/n$ in a mixture with $m_B = m_F$.

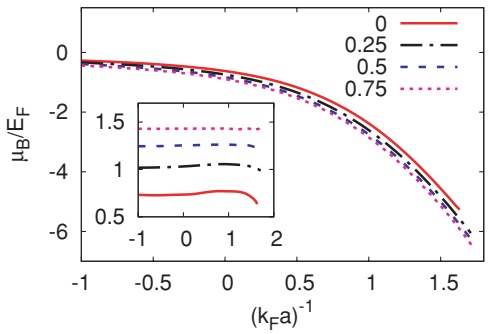

FIG. 3. (Color online) Boson chemical potential at the critical temperature T_c (in units of E_F) vs the boson-fermion coupling $(k_Fa)^{-1}$ for different values of the density imbalance $(n_F - n_B)/n$ in a mixture with $m_B = m_F$. The corresponding fermion chemical potential is reported in the inset.

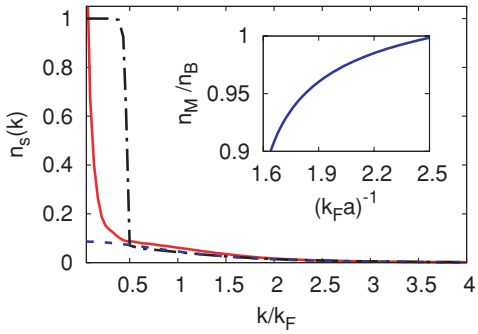

FIG. 4. (Color online) Boson (solid line) and fermion (dash-dotted line) momenta distribution curves for $n_B = n_F$, $m_B = m_F$, $(k_Fa)^{-1} = 1.63$, and $T = T_c \simeq 0.015E_F$. See text for the meaning of the dashed curve. The inset reports the fraction of molecules vs $(k_Fa)^{-1}$ for the same mixture at $T = 0.1E_F$.

that our equations coincide in this limit with those of Ref. [22] for the polaron-to-molecule transition, yelding the value $(k_Fa)^{-1} = 1.60$ for the critical coupling calculated within a corresponding T-matrix approximation [24,26]. The meeting of the properties of a Bose-Fermi mixture with those of a two-component Fermi mixture at this point of the phase diagram is quite remarkable, especially because, according to the results of Fig. 1, this "universal" point sets the scale for the quantum phase transition for *all* boson densities $n_B \leqslant n_F$. [27]

The chemical potentials μ_B and μ_F at T_c vs $(k_Fa)^{-1}$ are reported in Fig. 3 for different values of the density imbalance. The two chemical potentials have quite different behaviors. The fermion chemical potential remains almost constant in the whole range of coupling considered; the boson chemical potential, on the other hand, diminishes quite rapidly with increasing coupling while depending little on the density imbalance. These different behaviors result from the concurrence of several factors. For weak coupling, the increasing (negative) mean-field shift of the fermion chemical potential for increasing coupling is partially compensated by the decrease of the temperature when moving along the critical line. On the molecular side, the fermion chemical potential is instead determined by the Fermi energy of the unpaired fermions plus a mean-field shift caused by interaction with molecules. Pauli repulsion makes this interaction repulsive [4,18], thus keeping the fermion chemical potential positive. The boson chemical potential, on the other hand, interpolates between the mean-field value $2\pi n_F a/m_r$ in weak coupling and $\mu_B \approx -\epsilon_0$ in strong coupling, as required by molecule formation.

Figure 4 reports the momentum distributions $n_B(\mathbf{k})$ and $n_F(\mathbf{k})$ [as obtained before momentum integration in Eqs. (5) and (6)] at T_c, for a mixture with $n_B = n_F$, at the coupling value $(k_Fa)^{-1} = 1.63$ (approximately at the quantum critical point). The two distributions are markedly different at low momenta, consistent with their different statistics, but coalesce into the same behavior just after the step in the fermion momentum distribution. This common behavior corresponds to the function $n_M|\phi(\mathbf{k})|^2$ (dashed line in Fig. 4), where $\phi(\mathbf{k}) = (8\pi a^3)^{1/2}/(\mathbf{k}^2a^2 + 1)$ is the normalized two-body internal wave function of the molecules, while the coefficient n_M represents their density. In the present case $n_M = 0.89\,n_B$, showing that a fraction of bosons remains unpaired but still does not condense even at such a low temperature, corresponding to quite an unconventional Bose liquid. The fraction of unpaired fermions is instead more conventional and consists of a Fermi liquid, which is responsible for the jump in the fermion momentum distribution. In particular, the position of the jump in Fig. 4 at $|\mathbf{k}| \simeq 0.47\,k_F$, corresponds to an "enclosed" density of $0.10\,n_F$, in good numerical agreement with the value $0.11\,n_F$ obtained from the Luttinger theorem [28] for the fraction $(n_F - n_M)$ of unpaired fermions (using the value $n_M = 0.89\,n_B$ extracted independently previously). Note finally that the number of unpaired bosons progressively decreases by increasing the coupling, as expected on physical grounds, reaching eventually a 100% conversion of bosons into molecules, as shown in the inset of Fig. 4, where the ratio n_M/n_B is reported vs coupling at a constant temperature.

We conclude finally by commenting on three-body losses and mechanical instabilities that could prevent the experimental observation of the many-body physics described previously. The choice of restricting our analysis to mixtures with a majority of fermions was precisely aimed at reducing the importance of these nuisances. Three-body losses are dominated by processes involving two bosons and one fermion, with a rate proportional to $n_B^2 n_F$ [13]. They can thus be controlled by keeping n_B sufficiently small with respect to n_F. A predominance of fermions should also reduce the tendency to collapse, because of the stabilizing effect of Fermi pressure. As a matter of fact, we have verified that the compressibility matrix $\partial\mu_s/\partial n_{s'}$ remained positive definite for all couplings, temperatures, and densities $n_F \geqslant n_B$ considered in our calculations. Apparently, pairing correlations act to protect the system from the mean-field instabilities dominating the phase diagram of nonresonant Bose-Fermi mixtures. Resonant Bose-Fermi mixtures with a majority of fermions appear thus promising systems for the observation of a rich many-body physics.

We thank F. Palestini, A. Perali, and G. C. Strinati for a careful reading of the manuscript. Partial support by the Italian MIUR under Contract Cofin-2007 "Ultracold Atoms and Novel Quantum Phases" is acknowledged.

[1] L. Viverit, C. J. Pethick, and H. Smith, Phys. Rev. A **61**, 053605 (2000); R. Roth and H. Feldmeier, *ibid.* **65**, 021603(R) (2002); M. Lewenstein, L. Santos, M. A. Baranov, and H. Fehrmann, Phys. Rev. Lett. **92**, 050401 (2004).

[2] G. Modugno *et al.*, Science **297**, 2240 (2002).

[3] L. Radzihovsky, J. Park, and P. B. Weichman, Phys. Rev. Lett. **92**, 160402 (2004).

[4] M. Y. Kagan, I. V. Brodsky, D. V. Efremov, and A. V. Klaptsov, Phys. Rev. A **70**, 023607 (2004).

[5] A. Storozhenko, P. Schuck, T. Suzuki, H. Yabu, and J. Dukelsky, Phys. Rev. A **71**, 063617 (2005).

[6] S. Powell, S. Sachdev, and H. P. Buchler, Phys. Rev. B **72**, 024534 (2005); D. B. M. Dickerscheid, D. vanOosten, E. J. Tillema, and H. T. C. Stoof, Phys. Rev. Lett. **94**, 230404 (2005); A. V. Avdeenkov, D. C. E. Bortolotti, and J. L. Bohn, Phys. Rev. A **74**, 012709 (2006); L. Pollet, C. Kollath, U. Schollwock, and M. Troyer, *ibid.* **77**, 023608 (2008).

[7] M. Rizzi and A. Imambekov, Phys. Rev. A **77**, 023621 (2008); T. Watanabe, T. Suzuki, and P. Schuck, *ibid.* **78**, 033601 (2008).

[8] F. M. Marchetti, C. J. M. Mathy, D. A. Huse, and M. M. Parish, Phys. Rev. B **78**, 134517 (2008).

[9] I. Titvinidze, M. Snoek, and W. Hofstetter, Phys. Rev. B **79**, 144506 (2009).

[10] K. Günter, T. Stoferle, H. Moritz, M. Kohl, and T. Esslinger, Phys. Rev. Lett. **96**, 180402 (2006).

[11] C. Ospelkaus *et al.*, Phys. Rev. Lett. **97**, 120402 (2006).

[12] S. Ospelkaus, C. Ospelkaus, L. Humbert, K. Sengstock, and K. Bongs, Phys. Rev. Lett. **97**, 120403 (2006).

[13] J. J. Zirbel *et al.*, Phys. Rev. Lett. **100**, 143201 (2008).

[14] K.-K. Ni *et al.*, Science **322**, 231 (2008).

[15] S. Simonucci, P. Pieri, and G. C. Strinati, Europhys. Lett. **69**, 713 (2005).

[16] P. Pieri and G. C. Strinati, Phys. Rev. B **61**, 15370 (2000).

[17] See, e.g., V. N. Popov, *Functional Integrals and Collective Excitations* (Cambridge University Press, Cambridge, UK, 1987), Chap. 6.

[18] Details of the analytic calculations will be presented elsewhere (E. Fratini and P. Pieri, unpublished).

[19] Most of our calculations will be limited to the case $m_B = m_F$. This case, which is relevant for isotopic mixtures of sufficiently heavy atoms (^{39}K-^{40}K, e.g.), is taken as representative of the more general situation.

[20] N. V. Prokof'ev and B. V. Svistunov, Phys. Rev. B **77**, 125101 (2008).

[21] M. Veillette *et al.*, Phys. Rev. A **78**, 033614 (2008); P. Massignan, G. M. Bruun, and H. T. C. Stoof, *ibid.* **78**, 031602(R) (2008); C. Mora and F. Chevy, *ibid.* **80**, 033607 (2009); M. Punk, P. T. Dumitrescu, and W. Zwerger, *ibid.* **80**, 053605 (2009).

[22] R. Combescot, S. Giraud, and X. Leyronas, Europhys. Lett **88**, 60007 (2009).

[23] A. Schirotzek, C. H. Wu, A. Sommer, and M. W. Zwierlein, Phys. Rev. Lett. **102**, 230402 (2009).

[24] QMC calculations [20] and refined diagrammatic approximations [22] for the single spin-down problem yield the value $(k_F a)^{-1} = 1.11$ for the polaron-to-molecule transition, 30% off the T-matrix prediction. This difference is due to the overestimate of the molecule-fermion repulsion by the T-matrix approximation, which yields $8/3a$ for the molecule-fermion scattering length in place of the exact value $1.18a$ [25], thus making the molecule formation in a Fermi sea enviroment less convenient.

[25] G. V. Skorniakov and K. A. Ter-Martirosian, Zh. Eksp. Teor. Fiz. **31**, 775 (1956) [Sov. Phys. JETP **4**, 648 (1957)].

[26] The value 1.60 for the critical coupling in the limit $n_B \to 0$ is reached with a weak re-entrant behavior of the critical coupling vs imbalance, occurring at imbalances larger than those reported in Fig. 1.

[27] Our preliminary calculations for $m_B \neq m_F$ indicate that also in this case the critical coupling for a single boson governs the quantum phase transition. In particular, at the experimentally relevant ratio $m_B/m_F = 87/40$, the critical coupling is in the range $1.3-1.5$ at finite boson densities, its value for a single boson being 1.28.

[28] J. M. Luttinger, Phys. Rev. **119**, 1153 (1960).